Simple Epidemic Models with Segmentation Can Be Better than Complex Ones

Geon Lee
KAIST AI
Daejeon, South Korea
geonlee0325@kaist.ac.kr

Se-eun Yoon
KAIST EE
Daejeon, South Korea
seeuny@kaist.ac.kr

Kijung Shin
KAIST AI & EE
Daejeon, South Korea
kijungs@kaist.ac.kr

ABSTRACT

Given a sequence of epidemic events, can a single epidemic model capture its dynamics during the entire period? How should we divide the sequence into segments to better capture the dynamics?

Throughout human history, infectious diseases (e.g., the Black Death and COVID-19) have been serious threats. Consequently, understanding and forecasting the evolving patterns of epidemic events are critical for prevention and decision making. To this end, epidemic models based on ordinary differential equations (ODEs), which effectively describe dynamic systems in many fields, have been employed. However, a single epidemic model is not enough to capture long-term dynamics of epidemic events especially when the dynamics heavily depend on external factors (e.g., lockdown and the capability to perform tests).

In this work, we demonstrate that properly dividing the event sequence regarding COVID-19 (specifically, the numbers of active cases, recoveries, and deaths) into multiple segments and fitting a simple epidemic model to each segment leads to a better fit with fewer parameters than fitting a complex model to the entire sequence. Moreover, we propose a methodology for balancing the number of segments and the complexity of epidemic models, based on the Minimum Description Length principle. Our methodology is **(a) Automatic:** not requiring any user-defined parameters, **(b) Model-agnostic:** applicable to any ODE-based epidemic models, and **(c) Effective:** effectively describing and forecasting the spread of COVID-19 in 70 countries.

ACM Reference Format:
Geon Lee, Se-eun Yoon, and Kijung Shin. 2021. Simple Epidemic Models with Segmentation Can Be Better than Complex Ones. In *epiDAMIK 2021: 4th epiDAMIK ACM SIGKDD International Workshop on Epidemiology meets Data Mining and Knowledge Discovery.* ACM, New York, NY, USA, 8 pages. https://doi.org/xx.xxxx/xxxxxxxxx.xxxxxxx

1 INTRODUCTION

Infectious diseases have been serious threats to global public health. They not only change lifestyles of millions of people worldwide but also bring about dramatic changes in many areas, including economies, cultures, ecologies, and more. Unfortunately, the war against infectious diseases has continued throughout human history. The Black Death killed a third of the world's population in 1340s, and the Spanish flu in 1918 is estimated to have resulted in at most 500 million deaths. Recent epidemic outbreaks of SARS, Ebola, Zika, and COVID-19 show that the war is not over yet.

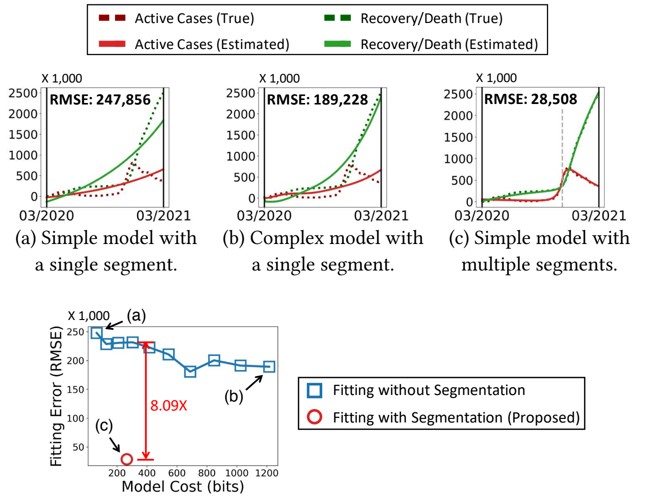

(a) Simple model with a single segment.
(b) Complex model with a single segment.
(c) Simple model with multiple segments.

(d) Trade-off between model complexity and data fitness.

Figure 1: Proper segmentation helps concisely and accurately describe the spread of COVID-19 in Italy. Dividing the event sequence (i.e., the numbers of active cases, recoveries, and deaths) properly into multiple segments and fitting a simple epidemic model to each segment leads to a more concise model with a better fit than fitting a complex model to the entire period. See the experiment section for details.

Consequently, understanding and predicting epidemic spreads are important for prevention and effective decision making. How many people will be infected within a week? How will lockdowns affect the spread? To answer these questions, we require a method that is simple enough to be comprehensible but expressive enough to accurately model and predict the spread of infectious diseases.

Ordinary differential equations (ODEs) have successfully described dynamic systems in various fields, including ecology, economics, physics, and biology. ODEs have also been utilized in epidemics. Some of the earliest epidemic models, such as SIS, SIR, and SEIR, are compartment models [10]. These models divide the population into several compartments and capture patterns of dynamic changes in the sizes of the compartments over time. The dynamics are expressed as predefined ODEs, which are based on human knowledge, with tunable parameters. While these models are intuitive and simple, they often have limited expressiveness,

epiDAMIK 2021, Aug 15, 2021, Virtual

ACM ISBN 978-1-xxxx-XXXX-X…$15.00
https://doi.org/xx.xxxx/xxxxxxxxx.xxxxxxx

failing to capture epidemic dynamics accurately. On the other hand, data-driven models [14, 15] aim to model and forecast co-evolving time-series data using ODEs, without relying on human knowledge. They employ latent variables and non-linear differential equations to capture complicated temporal dynamics.

Despite the development of epidemic models, describing long-term dynamics of epidemics using a single epidemic model often faces limitations due to the unpredictability and abruptness of real-world events. Indeed, various external factors may substantially change the dynamics of epidemic events. For example, policies reducing contacts between individuals (e.g., lockdown) and the capability to perform tests can significantly affect the dynamics.

In this work, we demonstrate that properly dividing an epidemic event sequence into multiple segments and fitting a simple epidemic model to each segment greatly helps describe and predict the epidemic propagation concisely and accurately. For example, in Figures 1(a) and (b), the entire sequence of events regarding COVID-19 in Italy is fitted to two epidemic models with different numbers of parameters. On the other hand, in Figure 1(c), the sequence is split into multiple segments, and then a simple model is fitted to each segment. As seen in Figure 1(d), the segmentation leads to 8.09× smaller fitting error with fewer parameters than using a single model for the entire sequence.

Then the following questions naturally arise: Given a sequence of epidemic events, where should we divide it? How many segments should we divide it into? We propose a segmentation scheme that greedily decides where to split. It also decides the number of segments by balancing the fitting error and the sizes of the models for all segments, based on the Minimum Description Length (MDL) principle.

We validate our approach using event sequences regarding recent Coronavirus Disease-19 (COVID-19), specifically the numbers of active cases, recoveries, and deaths in 70 countries. COVID-19 was recognized as a pandemic by the World Health Organization. By early April 2021, 129 million confirmed cases and 2.8 million deaths were reported worldwide. Our experiments reveal that our segmentation scheme enhances three epidemic models in explaining and predicting the propagation of COVID-19.

The strengths of our approach are summarized as follows:

- **Automatic:** It does not require any user-defined parameters, such as the number of segments.
- **Model-agnostic:** It is applicable to any ODE-based epidemic models without being restricted to certain models.
- **Effective:** Applied to the COVID-19 datasets, it significantly reduces the fitting error (up to 14.29× with fewer parameters) and forecasting error (up to 31.54×) of three epidemic models.

Reproducibility: The code and datasets used in the paper is available in [1].

2 RELATED WORK

We briefly review previous work on two related topics: epidemic models and time-series analysis models.

2.1 Epidemic Models.

A variety of epidemic models have been proposed to understand and predict the spread of infectious diseases [2]. In the SI model, the population is divided into two different groups: susceptible and infectious; and the size of each group changes based on predefined differential equations. Taking realistic conditions, such as reinfection, recovery, immunity, population change, and exposure, into consideration, the SI model has been extended to SIS, SIR [3], SIRS [9], SIRD [19], SEIR [8], and many more. The spread of COVID-19 has been analyzed using modified SIRs: [12] takes human mobility into account, and [6] considers quarantine controls. These models are intuitive, explainable, and simple since they are based on human knowledge. However, they show weakness in capturing long-term dynamics of epidemic events especially when the dynamics heavily depend on external factors. In this work, to the best of our knowledge, we adapt segmentation for the first time to epidemic models and empirically show its effectiveness in capturing and forecasting epidemic dynamics.

2.2 Time-series Analysis Models.

Mining and modeling time-series data is a building block of many analytical and predictive tasks, such as pattern discovery [20, 21], disaggregation [27], and forecasting [11, 14, 15, 17], in a variety of fields, including social media [13, 18], web [17], and medical science [7]. Especially, ordinary differential equations (ODEs) have attracted much attention, due to its simplicity and expressiveness, and [5, 22, 23, 26] focus on learning ODEs from data. Recently, [5] introduces a generative model to solve ODEs using neural networks. There have been several studies on learning to segment temporal data [11, 14–16]. [14, 15] slide a fixed sized window and incrementally forecast co-evolving events based on repeated patterns. While this approach can be effective in real-time forecasting, it fails to capture long-term patterns, especially when the window size is not large enough. We show in the experiment section that our segmentation scheme leads to 3.23× smaller fitting error, with the same number of parameters, than the segmentation method inspired by [14]. More importantly, the previous studies focus on detecting repetitive patterns in activities (e.g., sensor data and motion events), while we focus on segmenting epidemic data, where dynamics suddenly change due to external factors, and eventually better modeling and forecasting the spread of COVID-19.

3 PRELIMINARIES

In this section, we introduce some notations and three main epidemic models that are used in the paper. Refer to Table 1 for the frequently-used notations. We first review the Susceptible-Infectious-Recovered (SIR) model, which is one of the most classical compartment models. Then, we introduce two latent dynamics models that are based on linear and non-linear dynamics of latent variables.

3.1 Susceptible-Infectious-Recovered (SIR) Model

The SIR model is one of the most classical epidemic models. Given a group of individuals of closed population P, each individual is assigned to one of the three states: S (susceptible), I (infectious), and R (recovered). Here, we use $S(t)$, $I(t)$, and $R(t)$ to denote the number of individuals at the three states, respectively, at timestamp t. The model assumes that each individual goes through two types

Table 1: Frequently-used notations and symbols.

Notation	Definition
$x(t)$	observed epidemic event at time t
$v(t)$	estimated epidemic event at time t
$X = (x(1), \cdots, x(n))$	observed epidemic event sequence
$V = (v(1), \cdots, v(n))$	estimated epidemic event sequence
n	length of X
d	dimension of $x(t)$
β	infection rate
γ	recovery rate
$S(t)$	susceptible population at time t
$I(t)$	infected population at time t
$R(t)$	recovered population at time t
P	population of the region
$w(t)$	latent factors at timestamp t
k	number of latent factors
$Cost(M)$	description cost of model M
$Cost(X\|M)$	encoding cost of data X given model M
$Cost(X)$	total cost of X
f	solver for an epidemic model
r	number of segments
$X_{s_1:e_1} \oplus \cdots \oplus X_{s_r:e_r}$	segmentation of X into r segments

of transitions: infection and recovery. That is, the state to which an individual belongs changes from S to I and then from I to R. Additionally, the model assumes that the probability of a susceptible individual to get infected at each time t is proportional to the number of infected individuals with a coefficient β, and the model assumes that the probability of an infected individual to become recovered at each time t is γ. These dynamics can be expressed as the following three differential equations, where β and γ are model parameters:

$$\frac{\mathrm{d}S(t)}{\mathrm{d}t} = -\frac{\beta}{P} \cdot S(t)I(t),$$

$$\frac{\mathrm{d}R(t)}{\mathrm{d}t} = \gamma \cdot I(t),$$

$$\frac{\mathrm{d}I(t)}{\mathrm{d}t} = \frac{\beta}{P} \cdot S(t)I(t) - \gamma \cdot I(t).$$

Note that these equations imply $S(t) + I(t) + R(t) = P$.

3.2 Non-Linear Latent Dynamics (NLLD) Model

This model [14] consists of two multi-dimensional event sequences: a k-dimensional latent (i.e., unobservable) event sequence $w(t)$ and a d-dimensional observable event sequence $v(t)$. The observed events $v(t)$ are assumed to be determined by the following *non-linear* dynamical systems of the latent factors $w(t)$:

$$\frac{\mathrm{d}w(t)}{\mathrm{d}t} = p + Q \times w(t) + A \odot (w(t) \odot w(t)), \tag{1}$$

$$v(t) = u + V \times w(t), \tag{2}$$

where $\odot$ denotes the Hadamard product (i.e., the elementwise product); and $p \in \mathbb{R}^k$, $Q \in \mathbb{R}^{k \times k}$, and $A \in \mathbb{R}^k$ describe the linear, exponential, and non-linear dynamics between latent factors. In addition, $u \in \mathbb{R}^d$ and $V \in \mathbb{R}^{d \times d}$ are used to project the latent factors to the observed events. The model parameters are p, Q, A, u, V, and the initial condition $w(0) = w_0$ of the latent factors.

3.3 Linear Latent Dynamics (LLD) Model

We also consider a special case of the NLLD model, where the d-dimensional observed event sequence $v(t)$ is assumed to be determined by the following *linear* dynamical systems of k-dimensional latent factors $w(t)$:

$$\frac{\mathrm{d}w(t)}{\mathrm{d}t} = p + Q \times w(t),$$

$$v(t) = u + V \times w(t).$$

The NLLD and LLD models can naturally be used as epidemic models if we regard $I(t)$ and $R(t)$ (i.e., the numbers of infected and recovered individuals) in the SIR model as the 2-dimensional observed event sequence $v(t)$. Unlike the SIR model, the latent dynamics models are fully data driven, and thus they capture the temporal patterns in the event sequences without any prior knowledge of epidemics. Moreover, they describe the dynamics of the observed events using latent factors, which are not directly observed. Many real-world events are known to be largely affected by latent factors, and as shown in the experiment section, the latent dynamic models predict the spread of COVID-19 significantly more accurate than the SIR model.

Remarks: Our segmentation scheme described in the following section is model agnostic. That is, it can be applied to any epidemic or time-series analysis models, including but not limited to the three considered ones.

4 PROPOSED METHOD

In this section, we present our approach for deciding the number of segments and their locations automatically without user-defined parameters. We first define the description length of an event sequence. Then, based on the definition, we describe how we adapt the Minimum Description Length (MDL) principle to evaluate segmentation. Then, we propose a search algorithm for finding the best segmentation.

4.1 Description Length

Given a sequence X and a model M, the description length (in bits) of X, denoted by $Cost(X)$, is defined as:

$$Cost(X) := Cost(M) + Cost(X|M)$$

where the model cost $Cost(M)$ is the number of bits required to describe the model M, and the data cost $Cost(X|M)$ is the number of bits to encode X given M. The model cost and the data cost are described below.

4.1.1 Model Cost. To measure the model cost $Cost(M)$, we examine the parameters of the model M and their sizes in bits. Below, we consider the three aforementioned epidemic models. Note that the model cost of any other models can be measured in a similar way.

- **SIR Model:** The infection rate β and the recovery rate γ are two real numbers, and encoding each requires C_F bits.[1] Thus, the

[1] We set C_F to 8 by convention.

Algorithm 1: SEGMENT: MDL-based Greedy Segmentation Search

```
Input  : (1) epidemic event stream $X_{1:n}$
         (2) epidemic model solver $f$
Output : segmented event stream $X_{s_1:e_1} \oplus \cdots \oplus X_{s_r:e_r}$
1 if $n \leq 2$ then return $X_{1:n}$                              ▷ Base Case
2 $C \leftarrow Cost(f(X_{1:n})) + Cost(X_{1:n}|f(X_{1:n}))$
3 $i^* \leftarrow \underset{i \in \{2,\cdots,n-2\}}{\arg\min}\ Cost(X_{1:i} \oplus X_{i+1:n})$      ▷ Eq. (4)
4 $C^* \leftarrow Cost(X_{1:i^*} \oplus X_{i^*+1:n})$
5 if $C^* \geq C$ then return $X_{1:n}$
6 else return SEGMENT$(X_{1:i^*}, f) \oplus$ SEGMENT$(X_{i^*+1:n}, f)$
7                                                            ▷ Recursive Calls
```

model cost required to describe the SIR model in bits is:[2]

$$Cost(M) = 2 \cdot C_F.$$

- **Non-linear Latent Dynamics (NLLD) Model:** This model is described by a set of six parameters: w_0, p, Q, A, u, and V (see Eq. (1) and Eq. (2)). They contain to k, k, k^2, k, d, and kd real-valued parameters, respectively. Thus, the model cost in bits required to describe the NLLD model is:
$$Cost(M) = (k^2 + (3 + d) \cdot k + d) \cdot C_F. \tag{3}$$
- **Linear Latent Dynamics (LLD) Model:** The model cost required by the LLD model is:
$$Cost(M) = (k^2 + (2 + d) \cdot k + d) \cdot C_F.$$
Note that the cost in bits required to encode A is subtracted from Eq. (3).

4.1.2 Data Cost. The data cost $Cost(X|M)$ is the number of bits required to describe X given M. We assume the Huffman coding [4] to encode the difference between the observed event sequence X and the event sequence V estimated by the model M. Then, the number of bits required is the negative log-likelihood under a Gaussian distribution $\mathcal{N}(0, \sigma^2)$ as follows[3]:

$$\begin{aligned} Cost(X|M) &= -\log P(X - V) \\ &= -\log \prod\nolimits_{t=1}^{n} \prod\nolimits_{i=1}^{d} \frac{1}{\sqrt{2\pi\sigma^2}} e^{-\frac{(x_i(t)-v_i(t))^2}{2\sigma^2}} \end{aligned}$$

where $x_i(t)$ and $v_i(t)$ are the i-th dimension of actual and estimated events at time t.

4.2 Segmentation Evaluation

We adapt the Minimum Description Length (MDL) principle [25] for segmentation evaluation. Consider an event sequence $X (= X_{1:n})$ and a solver f of an epidemic model. We denote the division of X into r segments where each i-th segment starts at time s_i and ends at time e_i by

$$X_{s_1:e_1} \oplus \cdots \oplus X_{s_r:e_r},$$

where $s_1 = 1$, $e_r = n$, and $e_i + 1 = s_{i+1}$ for each $i \in \{1, \cdots, r-1\}$. Let $f(X_{i:j})$ be the epidemic model fitted to the segment $X_{i:j}$. Then, the description length in bits of $X_{s_1:e_1} \oplus \cdots \oplus X_{s_r:e_r}$ is:

$$\begin{aligned} Cost(X_{s_1:e_1} \oplus \cdots \oplus X_{s_r:e_r}) &= (r-1) \cdot \log_2(n) \\ &+ \sum_{i=1}^{r} \left(Cost(f(X_{s_i:e_i})) + Cost(X_{s_i:e_i} | f(X_{s_i:e_i})) \right), \end{aligned} \tag{4}$$

where $(r-1) \cdot \log_2(n)$ is the cost in bits required to encode $r-1$ splitting points (i.e., $s_2, \cdots, s_r$). Since each splitting point is an positive integer smaller than n, the number of bits required to encode it is $\log_2(n)$. The description length (i.e,. Eq. (4)) balances the fitting error and the size of the parameters required to encode the epidemic models for all segments, and we use it to evaluate segmentation. Specifically, based on the MDL principle, we prefer the segmentation that minimizes Eq. (4), and in the following subsection, we discuss how we search for such a segmentation.

4.3 Segmentation Search

Given an event sequence X, how can we find the segmentation that minimizes the description length (i.e., Eq. (4))? Since there are 2^n ways to segment a length n sequence, naïvely trying all possible segments is computationally prohibitive. Thus, we propose to greedily segment the sequence, as described in Algorithm 1, throughout which we make the length of each segment at least two. Given an event sequence $X_{1:n}$, we find a splitting point $i^* \in \{2, \cdots, n-2\}$ where the description length (i.e., Eq. (4)) of the corresponding segmentation is minimized (Line 3). If splitting $X_{1:n}$ at time i^* strictly decreases the description length, we divide $X_{1:n}$ into $X_{1:i^*}$ and $X_{i^*+1,n}$, and then recursively divide each segments (Line 6). Otherwise, we stop segmentation (Line 5). In the experiment section, we show that our greedy segmentation scheme outperforms baseline with up to 14.29× smaller fitting error with the same number of parameters.

5 EXPERIMENTS

In this section, we review our experiments designed to answer the following questions:

- **Q1. Effectiveness of Segmentation:** Does segmentation help understand the spread of COVID-19? Does it give a better trade-off between model complexity and fitness?
- **Q2. Effectiveness of our Segmentation Scheme:** How well does our greedy segmentation algorithm based on the MDL principle work? Does it yield small fitting error with the same number of segments than baseline?
- **Q3. Accuracy of Forecasting:** Is segmentation beneficial for accurately predicting the spread of COVID-19? Is it beneficial regardless of epidemic models used?

5.1 Experimental Settings

- **Machines:** We conducted all the experiments on a machine with AMD Ryzen 9 3900X CPU and 128GB RAM.
- **Datasets:** We considered the 70 countries with the most confirmed cases as of the end of March, 2021. We used the number of active cases as $I(t)$ and the number of recoveries and deaths

[2] We ignore the cost required to encode the population P since it is required only once regardless of the number of segments.

[3] We fix σ to the standard deviation of the elements of $X - V$ during the period of each segment..

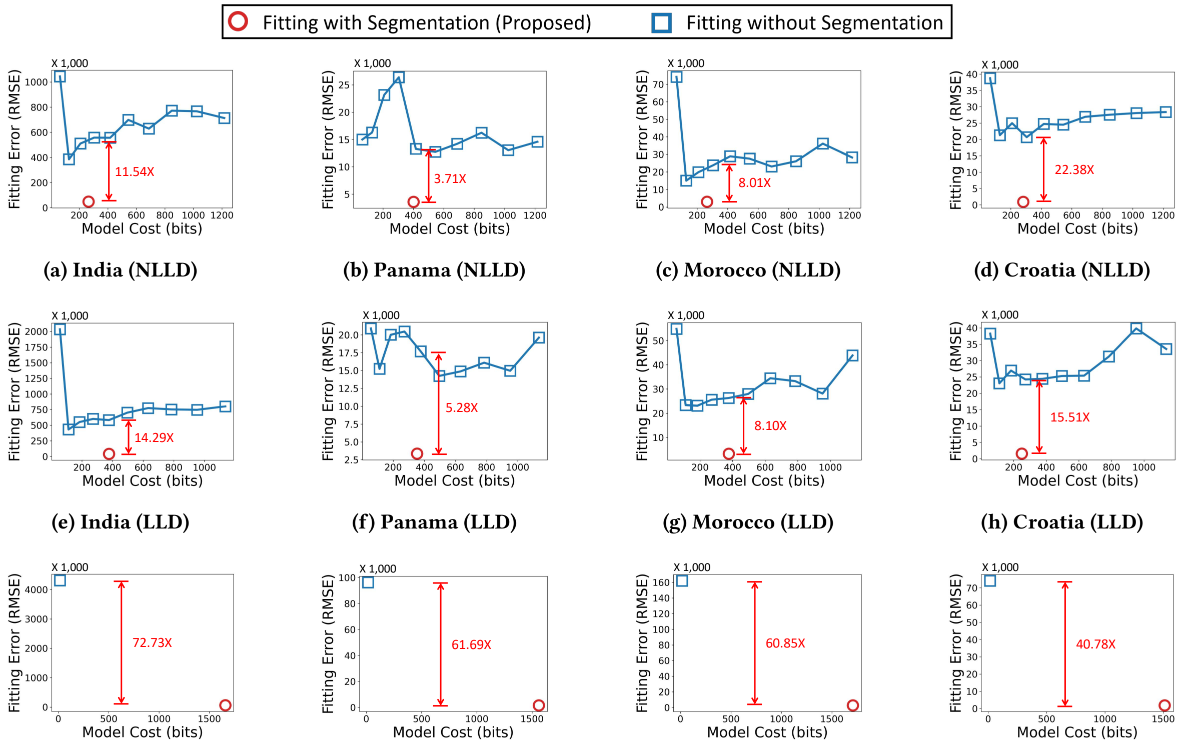

(a) India (NLLD) (b) Panama (NLLD) (c) Morocco (NLLD) (d) Croatia (NLLD)

(e) India (LLD) (f) Panama (LLD) (g) Morocco (LLD) (h) Croatia (LLD)

(i) India (SIR) (j) Panama (SIR) (k) Morocco (SIR) (l) Croatia (SIR)

Figure 2: Segmentation leads to better trade-offs between model complexity and fitting error. For the LLD and NLLD models without segmentation, k varies from 1 to 10.

as $R(t)$ in each of the 70 countries from March 1, 2020 to March 30, 2021. The dataset is publicly available at [24].[4]

- **Implementations:** We implemented the SIR model, the LLD model, and the NLLD model in Python. We used the Levenberg-Marquardt algorithm for optimization.
- **How to choose k:** For the LLD and NLLD models, we chose the number of latent factors k between 1 and 6 so that the description length (i.e., Eq. (4)) is minimized.

5.2 Q1. Effectiveness of Segmentation

We measure how segmentation by Algorithm 1 affects the model complexity and fitting error of the three considered epidemic models. As seen in Figure 2, segmentation leads to significantly better trade-offs between the model cost (in bits) and the fitting error (in terms of RMSE), regardless of the epidemic models used. For example, in the India dataset, the NLLD model with segmentation yields 11.54× smaller fitting error with smaller model cost than the same model without segmentation. Figure 3 show the input and estimated event sequences when the description length is minimized. The description length is minimized when a simple epidemic model with few latent factors is used with an enough number of segments. **Simple epidemic models with segmentation provide more concise and accurate description of the spread of COVID-19 than complex models without segmentation.** The results in the other countries can be found in the supplement [1].

5.3 Q2. Effectiveness of Our Segmentation Scheme

We demonstrate the effectiveness of our greedy segmentation scheme based on the MDL principle by comparing it with the incremental method inspired by [14]. The incremental method goes through the sequence from the start and initiates a new segment whenever the fitting error within the current segment exceeds a given threshold ϵ. As in [14], we set the threshold proportional to the L_2 norm of the current segment X_c with a coefficient α. That is, $\epsilon = \alpha \cdot ||X_c||_2$. Note that smaller α is expected to yield more segments. As seen in Figure 4, where we fix k to 2 and vary α from 0.05 to 0.5, our proposed segmentation scheme significantly outperforms the incremental method. Specifically, our scheme gives up to 3.23× smaller fitting error with the same model cost, which is proportional to the number of segments, than the incremental segmentation. The results in the other countries can be found in the supplement [1].

5.4 Q3. Accuracy of Forecasting

We examine the effect of segmentation on the the accuracy of future prediction using the three considered epidemic models. To this end, we divide each sequence into the training sequence and the test sequence, which span 327 days and 37 days, respectively. Then, we fit the epidemic models to each training sequence with and without segmentation and predict the event sequence during the test period. When segmentation is applied, for stable prediction, we ensure that

[4] Since the number of recoveries in the US is not available, we used the number of deaths as $R(t)$.

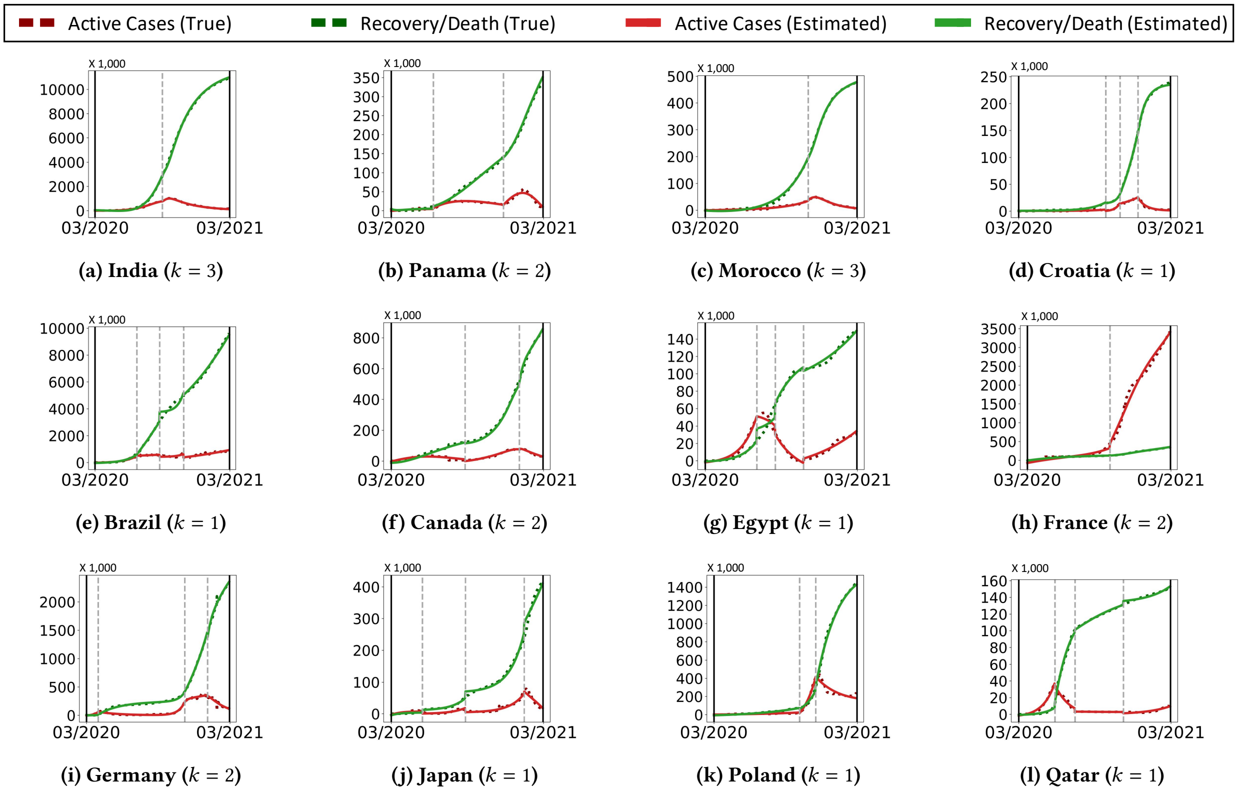

(a) India ($k = 3$) **(b) Panama** ($k = 2$) **(c) Morocco** ($k = 3$) **(d) Croatia** ($k = 1$)

(e) Brazil ($k = 1$) **(f) Canada** ($k = 2$) **(g) Egypt** ($k = 1$) **(h) France** ($k = 2$)

(i) Germany ($k = 2$) **(j) Japan** ($k = 1$) **(k) Poland** ($k = 1$) **(l) Qatar** ($k = 1$)

Figure 3: Simple models with multiple segments are preferred over complex models without segments. The true and estimated event sequences when the description length in bits is minimized.

the last segment is at least as long as the test period,[5] and we use the model fitted to the last segment of the training sequence for prediction. For the LLD and NLLD models without segmentation, we vary the the number of latent factors k from 1 to 6.

In Table 2, we compare the prediction error (in terms of RMSE) of the three epidemic models with and without segmentation. When the LLD model or the NLLD model is used, among 7 different settings, our segmentation scheme leads to the most accurate prediction in 32 and 33 (out of 70) countries, respectively. The second best one, which is the LLD model with $k = 2$ and no segmentation, is most accurate only in 9 countries. When the SIR model is used, segmentation increases the prediction accuracy in 70 (out of 70) countries. Moreover, prediction without segmentation is unstable with unreasonably large RMSE in some countries, while it is stable with segmentation in all countries. **To sum up, segmentation tends to improve the prediction accuracy of all three considered epidemic models.**

Note that with segmentation, only the last segment, not the entire sequence, is used for prediction. Despite the fact, segmentation increases the accuracy of prediction by letting epidemic models focus on the part that represents the current epidemic dynamics while ignoring the part before inherent changes in the dynamics.

6 CONCLUSIONS

In this work, we propose to divide epidemic event sequences into multiple segments and fit a simple model to each segment. To this end, we propose a greedy algorithm based on the MDL principle to decide where to split the sequences. Through extensive experiments using the COVID-19 event sequences from 70 countries, we demonstrate that our methodology has the following advantages:

- **Automatic:** All parameters are tuned automatically based on the MDL principle without relying on users.
- **Model-agnostic:** Any ODE-based epidemic models can be used with our segmentation scheme.
- **Effective:** The fitting error and prediction error of three epidemic models decrease up to 14.29× and 31.54×, respectively, with our segmentation scheme.

Reproducibility: The code and datasets used in the paper is available in [1].

REFERENCES

[1] 2021. Code, Data, and Online Appendix. https://github.com/geonlee0325/covid_segmentation.

[2] Roy M Anderson, B Anderson, and Robert M May. 1992. *Infectious diseases of humans: dynamics and control.* Oxford university press.

[3] Nino Antulov-Fantulin, Alen Lančić, Hrvoje Štefančić, and Mile Šikić. 2013. FastSIR algorithm: A fast algorithm for the simulation of the epidemic spread in large networks by using the susceptible–infected–recovered compartment model. *Information sciences* 239 (2013), 226–240.

[4] Christian Böhm, Christos Faloutsos, Jia-Yu Pan, and Claudia Plant. 2007. Ric: Parameter-free noise-robust clustering. *TKDD* 1, 3 (2007), 10–es.

[5] We can ensure this by Algorithm 1 so that it never splits the training sequence during its last 37 days.

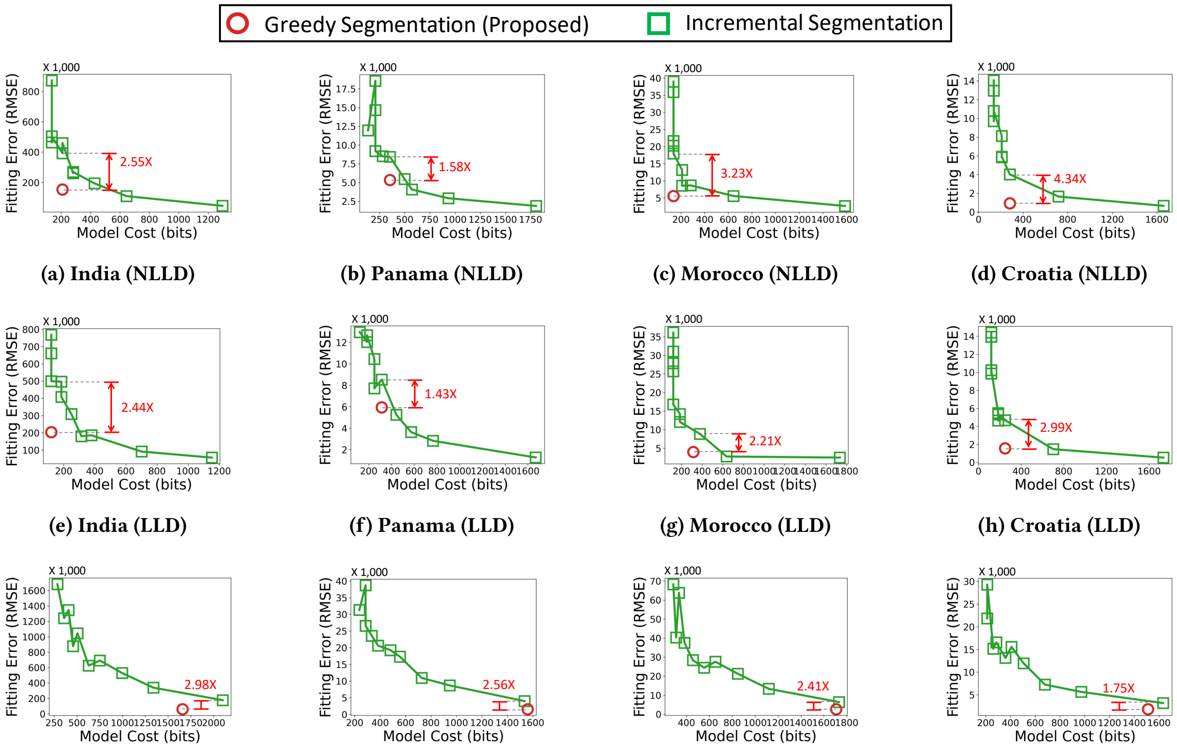

(a) India (NLLD) **(b) Panama (NLLD)** **(c) Morocco (NLLD)** **(d) Croatia (NLLD)**

(e) India (LLD) **(f) Panama (LLD)** **(g) Morocco (LLD)** **(h) Croatia (LLD)**

(i) India (SIR) **(j) Panama (SIR)** **(k) Morocco (SIR)** **(l) Croatia (SIR)**

Figure 4: Our proposed greedy segmentation scheme based on the MDL principle yields better segmentation than the incremental method.

[5] Ricky TQ Chen, Yulia Rubanova, Jesse Bettencourt, and David K Duvenaud. 2018. Neural ordinary differential equations. In *NeurIPS*.

[6] Raj Dandekar and George Barbastathis. 2020. Quantifying the effect of quarantine control in Covid-19 infectious spread using machine learning. *medRxiv* (2020).

[7] Ian Davidson, Sean Gilpin, Owen Carmichael, and Peter Walker. 2013. Network discovery via constrained tensor analysis of fmri data. In *KDD*.

[8] Haiping Fang, Jixiu Chen, and Jun Hu. 2006. Modelling the SARS epidemic by a lattice-based Monte-Carlo simulation. In *EMB*.

[9] Wenjuan Guo, Qimin Zhang, and Libin Rong. 2018. A stochastic epidemic model with nonmonotone incidence rate: Sufficient and necessary conditions for near-optimality. *Information Sciences* 467 (2018), 670–684.

[10] Herbert W Hethcote, Harlan W Stech, and Pauline van den Driessche. 1981. Periodicity and stability in epidemic models: a survey. In *Differential equations and applications in ecology, epidemics, and population problems*. Elsevier, 65–82.

[11] Bryan Hooi, Shenghua Liu, Asim Smailagic, and Christos Faloutsos. 2017. B eat L ex: Summarizing and Forecasting Time Series with Patterns. In *ECML-PKDD*.

[12] Ruiyun Li, Sen Pei, Bin Chen, Yimeng Song, Tao Zhang, Wan Yang, and Jeffrey Shaman. 2020. Substantial undocumented infection facilitates the rapid dissemination of novel coronavirus (SARS-CoV-2). *Science* 368, 6490 (2020), 489–493.

[13] Michael Mathioudakis, Nick Koudas, and Peter Marbach. 2010. Early online identification of attention gathering items in social media. In *WSDM*.

[14] Yasuko Matsubara and Yasushi Sakurai. 2016. Regime shifts in streams: Real-time forecasting of co-evolving time sequences. In *KDD*.

[15] Yasuko Matsubara and Yasushi Sakurai. 2019. Dynamic modeling and forecasting of time-evolving data streams. In *KDD*.

[16] Yasuko Matsubara, Yasushi Sakurai, and Christos Faloutsos. 2014. Autoplait: Automatic mining of co-evolving time sequences. In *SIGMOD*.

[17] Yasuko Matsubara, Yasushi Sakurai, and Christos Faloutsos. 2015. The web as a jungle: Non-linear dynamical systems for co-evolving online activities. In *WWW*.

[18] Yasuko Matsubara, Yasushi Sakurai, B Aditya Prakash, Lei Li, and Christos Faloutsos. 2012. Rise and fall patterns of information diffusion: model and implications. In *KDD*.

[19] Amenaghawon C Osemwinyen and Aboubakary Diakhaby. 2015. Mathematical modelling of the transmission dynamics of ebola virus. *Applied and Computational Mathematics* 4, 4 (2015), 313–320.

[20] Spyridon Papadimitriou, Jimeng Sun, and Christos Faloutsos. 2005. Streaming pattern discovery in multiple time-series. In *VLDB*.

[21] Spiros Papadimitriou and Philip Yu. 2006. Optimal multi-scale patterns in time series streams. In *SIGMOD*.

[22] Maziar Raissi and George Em Karniadakis. 2018. Hidden physics models: Machine learning of nonlinear partial differential equations. *J. Comput. Phys.* 357 (2018), 125–141.

[23] Maziar Raissi, Paris Perdikaris, and George Em Karniadakis. 2017. Numerical Gaussian processes for time-dependent and non-linear partial differential equations. *arXiv preprint arXiv:1703.10230* (2017).

[24] Sudalai Rajkumar. 2020. Novel Corona Virus 2019 Dataset. Day level information on covid-19 affected cases. https://www.kaggle.com/sudalairajkumar/novel-corona-virus-2019-dataset

[25] Jorma Rissanen. 1978. Modeling by shortest data description. *Automatica* 14, 5 (1978), 465–471.

[26] Michael Schober, David K Duvenaud, and Philipp Hennig. 2014. Probabilistic ODE solvers with Runge-Kutta means. In *NIPS*.

[27] Fan Yang, Hyun Ah Song, Zongge Liu, Christos Faloutsos, Vladimir Zadorozhny, and Nicholas Sidiropoulos. 2018. Ares: automatic disaggregation of historical data. In *ICDE*.

Table 2: Segmentation is helpful to accurate prediction of the spread of COVID-19. We compare the prediction error (in terms of RMSE, recorded in units of $1,000$) of each epidemic model equipped with our segmentation scheme ('ours') and the model without segmentation but with different numbers of latent factors.

	Linear Latent Dynamics (LLD)							**Non-linear Latent Dynamics (NLLD)**							**SIR**	
Country	**Single Segment ($r = 1$)**						**Ours**	**Single Segment ($r = 1$)**						**Ours**	**($r = 1$)**	**Ours**
	$k = 1$	$k = 2$	$k = 3$	$k = 4$	$k = 5$	$k = 6$		$k = 1$	$k = 2$	$k = 3$	$k = 4$	$k = 5$	$k = 6$			
Argentina	88.2	211.7	**52.4**	53.0	54.5	53.6	56.2	114.0	382.7	329.7	83.7	236.3	**39.6**	65.0	1,301.8	**107.4**
Armenia	43.4	16.3	17.1	16.4	12.8	13.8	**3.7**	38.5	43.0	30.5	10.2	32.6	12.3	**2.2**	115.1	**2.4**
Austria	40.0	45.0	22.8	37.7	20.6	48.6	**10.5**	39.3	74.0	106.7	26.7	68.7	21.1	**10.1**	291.9	**19.3**
Azerbaijan	65.8	125.6	40.2	40.1	40.1	37.4	**11.4**	41.5	37.2	46.8	43.1	40.5	39.7	**12.2**	161.4	**2.6**
Bangladesh	90.3	15.8	10.2	10.2	9.0	11.8	**6.6**	111.8	19.6	27.6	64.0	98.4	**11.7**	27.8	350.2	**6.5**
Belarus	73.4	10.1	10.4	7.8	5.3	5.9	**2.1**	11.5	49.0	73.4	19.9	**6.1**	6.8	6.2	177.7	**24.2**
Belgium	160.0	**16.5**	71.9	67.6	67.0	73.3	21.0	325.1	29.5	85.5	70.8	65.5	38.6	**11.6**	-	**29.4**
Bolivia	14.4	17.3	**3.5**	4.0	5.2	5.7	53.9	9.8	57.7	**3.3**	14.8	4.7	8.5	81.0	133.0	**30.0**
Brazil	289.0	242.8	116.6	120.2	118.5	**115.6**	177.6	223.9	542.7	621.4	193.6	523.3	215.3	**95.0**	6,252.0	**682.3**
Bulgaria	**71.3**	91.4	91.2	77.5	76.2	76.4	78.4	**78.3**	130.4	518.3	126.3	100.5	102.1	89.5	144.4	**13.5**
Canada	65.0	141.2	39.0	120.8	**25.5**	25.5	50.8	84.6	**43.6**	98.5	45.2	61.4	52.0	74.2	545.3	**68.1**
Chile	95.1	211.3	16.2	16.1	16.6	17.7	**13.3**	188.4	29.8	**17.3**	26.7	55.3	111.9	40.9	519.6	**60.9**
Colombia	483.3	94.8	84.8	84.1	82.5	**82.1**	110.0	365.5	602.0	118.0	93.9	**88.9**	97.6	158.3	1,470.1	**161.5**
Costa Rica	23.3	**4.4**	4.5	10.6	12.6	12.9	13.9	37.1	8.4	**6.2**	6.7	9.4	11.8	17.2	117.9	**9.8**
Croatia	61.7	22.3	41.7	26.3	22.6	22.5	**2.8**	104.5	38.5	64.6	32.1	48.6	39.8	**2.4**	164.7	**7.4**
Czech	145.8	**69.0**	71.6	105.7	110.2	109.6	71.8	114.9	172.0	206.8	110.3	**109.6**	111.0	118.1	678.2	**98.9**
Denmark	36.8	22.1	34.2	34.9	33.3	34.7	**11.7**	32.7	32.6	73.1	37.3	37.5	28.4	**19.8**	138.3	**8.8**
Dominican Rep.	9.9	**8.4**	9.8	9.8	9.9	9.3	17.5	11.0	**9.2**	10.8	10.8	9.2	11.2	17.5	127.2	**21.2**
Ecuador	40.0	11.7	10.8	11.0	12.2	11.4	**10.0**	64.3	11.5	11.9	17.1	11.1	11.4	**10.2**	167.2	**19.3**
Egypt	30.4	26.0	**7.7**	8.3	8.0	9.6	14.7	9.7	26.0	9.9	**8.1**	11.4	12.8	13.4	103.0	**8.4**
France	62.8	83.1	76.6	90.3	114.1	95.2	**41.8**	81.8	98.7	159.4	**66.0**	73.3	95.8	92.7	-	**250.4**
Georgia	34.3	26.1	83.4	40.3	29.1	30.1	**15.4**	45.5	64.1	74.1	59.2	38.2	91.4	**6.1**	182.1	**9.5**
Germany	467.4	72.0	71.1	72.5	71.6	72.5	**67.8**	591.2	98.7	180.5	326.0	160.7	104.6	**88.9**	1,513.3	**174.2**
Greece	12.9	14.4	16.3	18.2	17.9	18.7	**12.6**	13.7	16.6	18.8	15.7	18.4	17.9	**10.4**	85.6	**11.7**
Guatemala	38.6	**1.0**	1.0	1.1	1.1	1.3	3.1	32.6	36.3	16.9	**1.0**	23.9	1.1	19.4	110.7	**9.8**
Honduras	**5.7**	8.7	7.9	7.0	8.1	7.2	16.5	**5.1**	11.2	10.5	7.9	7.8	7.2	15.4	78.8	**12.1**
Hungary	119.8	71.0	30.3	**30.1**	30.6	30.4	53.2	168.9	97.7	46.4	34.8	46.7	39.3	**22.9**	218.2	**25.5**
India	3,517.9	145.8	180.3	430.2	590.6	705.5	**45.0**	1,629.2	142.9	278.4	315.5	242.9	424.0	**111.4**	7,571.9	**171.0**
Indonesia	**21.2**	32.7	30.3	23.3	25.7	27.1	45.5	27.3	51.8	28.9	24.9	24.3	**22.7**	70.7	719.7	**162.4**
Iran	271.7	63.5	70.3	70.1	70.4	67.7	**48.7**	182.4	228.1	1,982.8	81.5	76.7	72.5	**65.0**	944.9	**90.9**
Iraq	64.2	50.8	43.1	34.3	**31.7**	35.1	35.3	84.1	53.4	56.0	42.8	35.8	40.1	**27.2**	436.2	**20.6**
Ireland	88.7	55.4	55.3	56.0	17.5	**14.6**	33.7	71.9	76.3	76.4	13.6	13.5	18.0	**2.4**	119.4	**22.3**
Israel	35.3	22.1	21.5	**20.3**	22.1	26.4	131.7	47.4	121.6	19.6	**15.4**	19.9	20.9	87.8	451.3	**92.2**
Italy	459.8	806.5	318.1	362.5	349.1	245.8	**60.0**	550.8	426.8	320.7	321.7	245.8	362.3	**120.7**	1,611.9	**156.4**
Japan	65.1	64.8	**53.9**	54.1	55.2	56.5	82.6	76.4	74.3	67.1	64.9	**61.6**	63.3	77.6	261.5	**55.8**
Jordan	37.0	103.6	183.0	106.6	79.4	84.6	**11.8**	50.5	107.2	106.2	76.1	81.3	100.4	**13.6**	232.3	**17.9**
Kazakhstan	38.8	16.2	15.9	15.9	16.5	15.7	**5.0**	50.8	15.6	16.4	**8.1**	10.1	14.2	21.9	156.9	**18.5**
Kuwait	7.1	7.0	4.5	4.7	5.6	4.8	**3.5**	22.6	7.5	19.0	11.7	5.8	**4.8**	4.9	116.8	**9.9**
Lebanon	33.1	38.0	**31.5**	38.5	38.1	38.6	94.5	33.8	**26.0**	35.2	40.8	40.9	41.6	85.2	175.7	**64.1**
Lithuania	57.9	41.0	40.6	36.4	42.2	42.2	**29.1**	41.2	55.7	94.7	127.9	55.7	56.1	**28.7**	122.3	**11.1**
Malaysia	**14.4**	14.8	22.1	22.7	24.5	23.3	29.6	35.0	28.2	23.4	25.0	25.1	25.2	**21.2**	148.1	**53.3**
Mexico	135.8	75.8	78.2	**69.0**	69.6	77.8	97.9	144.5	71.8	73.5	76.6	70.7	**66.8**	81.9	1,192.0	**165.0**
Moldova	47.6	**5.9**	5.9	6.1	6.0	6.4	6.4	46.0	6.4	6.6	20.6	6.3	7.5	**5.2**	112.4	**9.0**
Morocco	85.3	13.9	14.0	15.1	17.2	16.3	**1.3**	61.5	62.2	111.7	22.3	19.9	87.1	**7.6**	328.3	**10.6**
Nepal	90.3	15.0	15.0	49.7	42.7	41.1	**4.9**	30.8	40.4	4.4	70.5	47.2	54.5	**3.0**	190.9	**2.8**
Netherlands	83.1	102.9	42.9	**37.8**	39.0	44.1	128.8	108.4	65.7	100.9	115.8	**41.6**	42.6	140.4	-	**55.2**
Pakistan	16.6	33.3	13.8	18.0	18.2	18.1	**3.5**	**9.2**	33.6	69.3	25.4	27.7	18.2	11.7	374.1	**25.0**
Panama	28.4	33.5	23.9	23.7	23.7	**23.4**	47.7	29.9	27.4	28.9	40.2	29.0	**26.7**	271.4	214.6	**23.8**
Paraguay	13.0	3.3	3.0	2.5	**1.8**	1.8	2.8	15.8	**3.7**	3.9	4.4	10.4	8.1	10.3	86.0	**10.9**
Peru	49.3	**43.3**	43.3	43.3	43.3	43.3	53.2	228.7	71.9	162.3	144.9	308.0	**39.7**	41.5	813.8	**93.8**
Philippines	157.4	53.1	39.1	38.7	35.6	14.4	**11.9**	89.2	78.3	119.0	12.5	39.0	24.5	**11.9**	361.1	**26.9**
Poland	218.1	119.4	100.9	94.3	89.1	97.6	**63.8**	168.8	208.6	71.1	79.0	92.3	72.4	**50.8**	970.4	**78.1**
Portugal	**58.7**	78.5	80.4	80.0	79.6	80.2	268.2	**54.3**	83.0	86.5	78.4	88.4	89.1	165.1	452.8	**144.1**
Qatar	24.2	10.8	5.6	6.7	5.5	6.9	**3.8**	34.0	16.6	5.4	5.4	12.8	5.8	**3.8**	104.8	**5.0**
Romania	119.4	55.6	71.8	57.9	72.9	74.7	**18.2**	180.4	142.1	91.6	72.1	120.0	83.4	**28.8**	505.9	**34.0**
Russia	443.7	56.9	187.5	182.3	176.9	279.9	**36.5**	243.0	540.5	**56.3**	99.1	167.3	924.9	266.1	2,507.5	**249.2**
Saudi Arabia	86.6	12.2	6.5	6.3	5.8	5.5	**3.6**	49.4	10.8	16.5	13.3	9.0	5.4	**5.2**	260.8	**4.1**
Serbia	224.7	240.3	**49.6**	169.1	167.0	167.0	78.7	87.5	42.2	**24.1**	136.6	151.3	138.8	104.8	289.9	**22.5**
Slovakia	55.2	20.8	30.2	22.1	**18.0**	19.9	31.4	52.2	**17.9**	59.2	21.7	54.3	19.2	20.0	172.1	**32.1**
Slovenia	46.8	**4.4**	18.5	10.3	26.5	26.7	5.7	19.7	9.2	26.3	21.7	30.1	39.0	**5.8**	113.6	**17.8**
South Africa	239.2	187.0	56.1	63.8	64.1	**41.3**	1,138.3	222.2	175.9	64.6	**52.0**	65.5	64.5	1,639.5	988.8	**76.2**
Spain	648.6	86.1	82.6	81.7	81.3	**81.2**	449.0	568.1	266.8	82.2	**72.8**	84.7	85.0	162.7	-	**379.2**
Sweden	57.0	48.4	46.1	46.2	**46.0**	46.2	133.9	69.8	**21.3**	44.6	43.1	57.3	56.6	185.9	-	**42.9**
Switzerland	88.1	84.0	83.2	84.1	84.5	83.2	**18.5**	66.7	91.6	88.2	82.8	90.6	91.6	**15.1**	274.1	**22.8**
Tunisia	22.6	**19.5**	19.5	19.7	20.5	20.4	27.4	24.0	24.2	**22.4**	23.2	23.2	22.9	56.4	130.7	**26.4**
Turkey	220.4	287.0	227.8	418.9	461.3	476.3	**144.4**	247.4	241.3	209.1	619.6	479.1	509.8	**177.2**	1,741.9	**98.4**
UAE	79.8	50.0	27.4	19.0	20.8	**18.6**	51.4	18.9	47.6	20.0	19.3	**14.6**	37.1	71.9	224.1	**52.8**
UK	**236.7**	363.8	510.5	432.3	360.7	355.7	821.7	**236.3**	606.8	576.0	785.8	457.7	639.5	963.0	-	**377.8**
Ukraine	287.4	130.7	105.0	109.9	103.2	108.5	**80.2**	373.9	186.8	220.0	150.2	106.4	196.2	**86.2**	813.1	**57.6**
US	137.8	144.7	134.1	134.4	132.0	**90.0**	134.9	139.9	117.1	148.0	196.2	160.6	123.7	**114.8**	-	**100.3**
No. Rank 1	6	9	6	4	5	8	**32**	5	6	6	7	6	7	**33**	0	**70**